JOURNAL OF CATALYSIS 121, 141–152 (1990)

Redispersion of Platinum on Pt/Al_2O_3 Model Catalyst in Oxygen Studied by Transmission Electron Microscopy

J. M. RICKARD,[1] L. GENOVESE, A. MOATA, AND S. NITSCHE

Centre de Recherche sur les Mécanismes da la Croissance Cristalline, CNRS, Campus de Luminy, Case 913, 13288 Marseille Cedex 09, France

Received December 22, 1987; revised June 30, 1989

A model Pt/Al_2O_3 catalyst was studied by transmission electron microscopy and Auger electron spectroscopy. O_2 treatments under industrial catalyst regeneration conditions (500°C, 20 Torr, 1 h) transform a monomodal distribution of Pt particles (mean diameter 18 Å) into a bimodal distribution consisting of a phase of particles 40 to 100 Å in diameter and a phase of very small clusters (diameter < 10 Å). This observation of stable small clusters is direct evidence for a Pt catalyst dispersion in O_2. Auger spectroscopy gives *in situ* information about particle transformation and support interaction. An exchange of matter between particles which operates on a molecular scale and might include platinum oxide is postulated.

INTRODUCTION

Much recent research has focused on model catalysts composed of metal particles on a ceramic support and on the changes which they undergo in a gaseous atmosphere. In the present study it was proposed to investigate the system Pt/Al_2O_3, because finely divided alumina with a small amount of platinum (less than 2% in weight) is widely used in industry as a reforming catalyst. Such catalysts are normally prepared by impregnating alumina with a soluble platinum compound. They are activated by air calcination followed by hydrogen reduction (*1–3*). These catalysts are subject to a process of "ageing," since long use in the presence of hydrocarbons or heating beyond 400°C in H_2 reduces their activity (*4–7*). This deactivation is attributable to poisoning (*8–10*) or to a decrease in the metal surface area through grain coalescence. These processes can be assessed either by measuring the metal surface area using H_2 or CO adsorption (*7*), by X-ray diffraction (*4*), or by microscopy (*11–13*).

On the other hand, it has been observed that an oxygen treatment at 500°C (followed or not by H_2 reduction at a lower temperature) can restore the initial activity of the catalyst (*3, 6*); with this procedure, which is known as regeneration of the catalyst, it is possible to recover the initial H_2 or CO adsorption capacity of the catalyst (*8, 12, 14, 15*). This reactivation cannot be explained only by the fact that the carbon deposits are removed by heat treatment. This phenomenon is called "redispersion" because the increase in the adsorbing capacity is generally correlated with an increase in the metal area, possibly resulting from the Pt on the support having broken up into smaller particles.

Whether or not an actual redispersion takes place under oxygen treatment remains an open question. Many investigators using transmission electron microscopy (TEM) have attempted to confirm and even to explain this point (*16–18*). With commercial catalysts, it is difficult to confirm this hypothesis by TEM because the smallest platinum grains would not be visible in the alumina powder due to lack of contrast, as shown in the following example (*19*). An H_2PtCl_6-impregnated alumina with 0.4% wt Pt was prereduced at 400°C. The particle size distribution showed that the mean diameter was $\bar{d}_{TEM} = 10$ Å in agree-

[1] Deceased.

0021-9517/90 $3.00

ment with hydrogen adsorption measurements ($\bar{d}_{ad}$ = 8 Å), assuming spherical particles and H/Pt = 1; heating in H_2 at 600°C led to $\bar{d}_{TEM}$ = 16 Å and $\bar{d}_{ad}$ = 28 Å by adsorption, which would be equivalent to an ageing by coalescence. This sample treated at 600°C in a mixture containing 3% O_2 in N_2 (under atmospheric pressure) was found by TEM to have undergone considerable coalescence, $\bar{d}_{TEM}$ = 200–2000 Å, but hydrogen adsorption measurements indicated that $\bar{d}_{ad}$ = 25 Å. Other authors using only hydrogen adsorption data (*14, 15*) have reported a decrease in $\bar{d}_{ad}$ occurring after treatment at around 500–550°C. The authors of another recent study (*12*) confirm this point and claim that under TEM the grains were found to have decreased in size and even to have vanished; however, this statement was not supported with histograms and so is not very convincing. The fact that oxygen produces a $\bar{d}_{ad}$ decrease and a $\bar{d}_{TEM}$ increase is a paradox which still needs to be elucidated.

Experiments on model catalysts (platinum deposited by evaporation onto thin alumina films) provide more favourable conditions for microscopy. A recent study (*20*) was carried out by the authors of Ref. (*19*) with similar initial grain diameters ($\bar{d}_{TEM}$ = 18 Å) and treatments, but without any measurement of the specific platinum surface area. Heating in H_2 at 500°C transformed $\bar{d}_{TEM}$ from 18 to about 40 Å. The coalescence was further increased by a subsequent treatment in O_2 at 500°C ($\bar{d}_{TEM}$ = 250 Å). The faceting of Pt crystallites was observed at 600°C and it was therefore concluded that a reactivating treatment in O_2 does not produce a redispersion of size, but on the contrary a much more active coalescence in O_2 than in H_2. Similar contradictory results have been reported by others authors (*21*). A possible explanation for this paradox may be as follows: an oxygen treatment reducing the total platinum area (coalescence) increases the activity, as observed elsewhere with hydrogen adsorption measurements, by creating active sites. Nevertheless, an alternative explanation is that measurements with the H_2 adsorption technique might detect platinum crystallites which were not revealed by TEM on a real catalyst.

In summary, the literature suggest that there may be several explanations for reactivation of Pt catalyst by oxygen treatment:

—removing of carbon contaminant
—creation of active sites
—formation of small Pt clusters.

The aim of this study was to observe and compare the behaviour of platinum crystallites obtained by evaporation onto an α-Al_2O_3 single crystal, as-deposited, during heating in H_2 and during heating in O_2. The pressure and temperature conditions (350–550°C, 1 Torr to 1 atm) were similar to those pertaining in industrial catalyst regeneration processes (1 Torr = 133.3 N m^{-2}). Auger electron spectroscopy (AES) was used to check the substrate purity and evaporation deposit. Similar (but thinner) substrates were simultaneously subjected to the same treatments and were subsequently observed under TEM. Granulometric distributions down to a size of 5 Å could thus be determined, and the crystallite morphological development observed. As reported below, an O_2 treatment was found to transform the monomodal distribution of platinum particles into a biomodal distribution. Many very small-sized clusters appeared simultaneously with large crystallites; this bimodality in size may help to resolve the apparent contradictions discussed above.

EXPERIMENTAL

Alumina substrates. Single crystals of $(10\bar{1}0)\alpha$-Al_2O_3 were polished with 0.5 μm diamond paste. The sample used for AES was a disk 8 mm in diameter. The plates for TEM, lamellas of (3 × 3) mm^2 × 50 μm, were prethinned from the backside around the center by ion-beam etching, until a small hole was formed; the edge of the hole was sufficiently thin for TEM. These lamel-

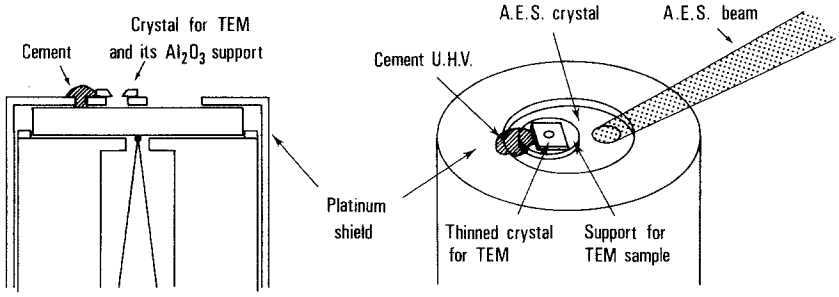

FIG. 1. Arrangement of the alumina crystals (for AES and TEM) on the heating holder.

las were each supported by a thick Al_2O_3 ring; both parts were movable and could be put either on the Al_2O_3 disk for the experiments or in the microscope.

Heating holder. The above two samples for AES and TEM were placed (as shown in Fig. 1) on a furnace made entirely of platinum, the insulator being pure alumina. A chromel–alumel thermocouple was applied against the rear face of the alumina disk; the front face temperature was standardized using data on the melting of various metal pellets. This furnace can operate in O_2 or H_2 atmospheres up to 600°C and in UHV, without producing any contamination.

Experimental preparations. The heating holder was placed at the end of a four-motions manipulator, in a UHV vessel (molecular and ionic pumps). Before the experiments, several tens of nanometers of the surface were removed by argon ion bombardment. An air lock leading to the UHV chamber was used as the treatment chamber. Heating at 550°C in 10^{-1} Torr O_2 was performed in this air lock until a clean surface for AES was obtained; in particular the carbon and sulphur Auger peaks therefore completely disappeared and only aluminium and oxygen peaks remained at the maximum intensity. These peaks were shifted by 3 eV by charge effect (48 and 500 eV) (*22, 23*); these positions were stable under the electron beam.

Platinum depositing and treatments. Platinum was evaporated onto crystals from a tungsten boat in UHV. Evaporation (from 0.3 monolayer at 1 Å/mn) was measured with a quartz microbalance (Q equivalent monolayers); the purity and surface coverage were monitored by AES. The two samples used for AES and TEM received the same deposits and treatments. After evaporation, the treatments in various gases (O_2, H_2, N_2) were carried out in the air lock, from 1 Torr up to 100 Torr, and from 350°C up to 550°C for 1 h (in the case of the present results). The absolute pressures were measured with a membrane gauge (Baratron) and the gas quality was checked with a mass spectrometer.

Transmission electron microscopy (TEM). The microscope used was a Jeol 100C, operating at 100 kV with a 500,000× magnification. The condenser aperture was 1 mrd, the spherical aberration coefficient was C_s = 1.7 mm, the objective lens aperture in reciprocal space was 0.34 or 0.23 $Å^{-1}$ radius; the latter allows only the specular beam to pass (by suppressing the Pt and Al_2O_3 diffracted electrons). The micrographs presented here were taken at about −1000 Å underfocus. The particle size distributions were measured from photographic enlargments, by visual counting with 1 Å resolution (the particle analyser was a Carl Zeiss TGZ_3). The error on the grain count, the mean diameter $\bar{d}_{TEM}$, and the surface fractional coverage in platinum θ_{TEM} were estimated to be less than 10, 15, and 20%, respectively (for grain sizes higher than 10 Å).

Auger electron spectroscopy. The equipment used was a four-grid analyser with a

45°C electron beam incidence (2 keV, 10 μA). The fractional surface area θ_A of platinum particles and the mean thickness of grains m_A (monolayer number) can be calculated from the normalized intensity J_d of the 153-eV Pt Auger signal, as a function of the Pt deposited (Q expressed in equivalent monolayers, E.ML). The simplest possible model of islands was used, namely homothetic square prisms, n atoms in side length, m atoms in thickness ($h = m/n$ = constant) and the graphic method given by Poppa and Soria (*24*) was used. For the attenuation factor of the adsorbate Auger peak (at 153 eV) through a monolayer of adsorbate, we found the value of $\alpha = 0.63 \pm 0.1$; this was compatible with the values of 0.54 and 0.58 for the 64-eV Pt Auger peak given in the literature (*25–27*).

RESULTS

1. Platinum Evaporation

Deposits at 200°C (Fig. 2a) show a diameter distribution with a Gaussian form, maximum at 16 Å, with a mean diameter $\bar{d} = 19$ Å. Some examples are given in Table 1. The values of the last column, Q_{TEM}, were obtained with the hypothesis that particle shape was hemispherical. They were clearly lower than values of Q measured with the quartz microbalance; this may be due partly to the condensation coefficient on Al_2O_3 being lower than that on the microbalance (coefficient $\simeq 1$). The values of this coefficient for other systems, Pd/MgO (*28*) or Au/NaCl (*29, 30*) vary from 0.2 to 0.5 (at 200–400°C). However, the estimated error in the reproducibility of the deposits was less than 20%.

At the practical level, it was possible in each experiment to measure by AES under vacuum the cleanliness and the Auger signal I_d of a given quantity of platinum Q. These measurements were performed just after deposit and after treatment. The sample was then removed from the vacuum chamber for TEM examination.

2. Heat Treatment under Vacuum H_2 and N_2

Annealing under vacuum for 1 h at 500°C did not produce any significant changes either in size distribution or in AES signal. No significant changes occurred either in Auger signals or in size distributions when the specimens were heated in N_2 (20 Torr) at 500°C or in H_2 (1 Torr) at 420°C (1 h). We could not perform these treatments at higher temperatures and higher pressures in H_2.

3. Heat Treatments in Oxygen

Table 2 and Figs. 2 and 3 show the overall results obtained with an amount of Pt $Q_{TEM} = 0.5$ monolayer. Very small clusters appeared under some conditions, and to make sure that these were produced by

TABLE 1

Deposits of Platinum Particles on Al_2O_3 Measured with Quartz Microbalance in Equivalent Monolayers Q and with Electron Microscopy (Q_{TEM}) Assuming Hemispherical Particles of Density ρ

Quartz microbalance Q	Electron microscopy			
	θ_{TEM}	$\bar{d}_{TEM}$ (Å)	ρ $\times 10^{12}$/cm^2	Q_{TEM} (1/2 sphere)
1.2	0.12	13	9	0.25
1.2	0.10	12	7	0.2
1.2	0.13	13	9	0.3
3	0.20	18.4	8	0.5
3	0.23	18	9	0.55

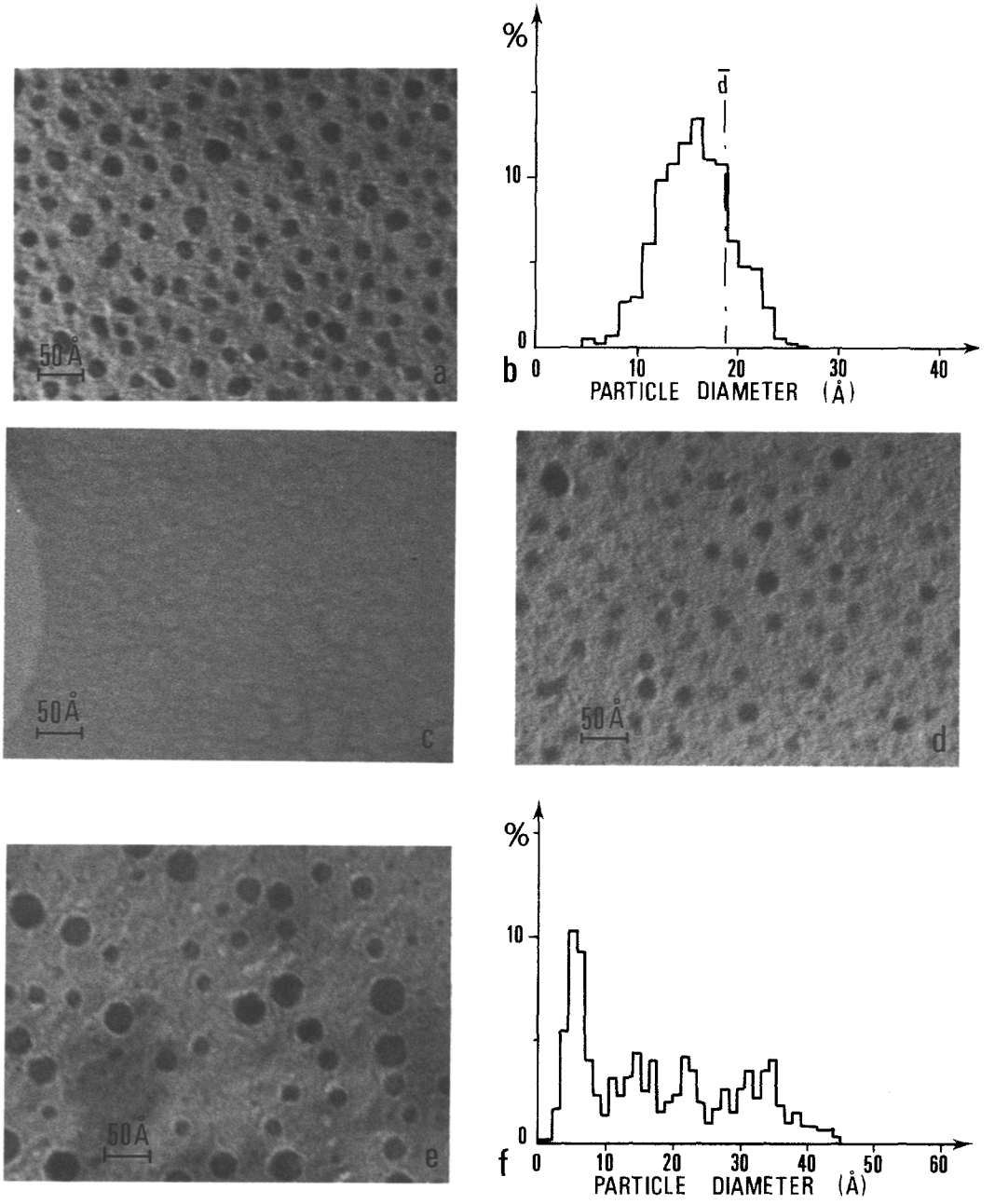

FIG. 2. Micrographs and corresponding size distributions of similar Pt/Al_2O_3 deposits ($Q_{TEM} \sim 0.5$). (a and b) Deposited at 200°C. (c) Al_2O_3 substrate cleaned under standard conditions, but without platinum deposit, then treated in O_2 (20 Torr, 500°C, 1 h). (d) Deposit treated in O_2 (20 Torr, 420°C, 1 h). (e and f) Deposit treated in O_2 (1 Torr, 550°C, 1 h).

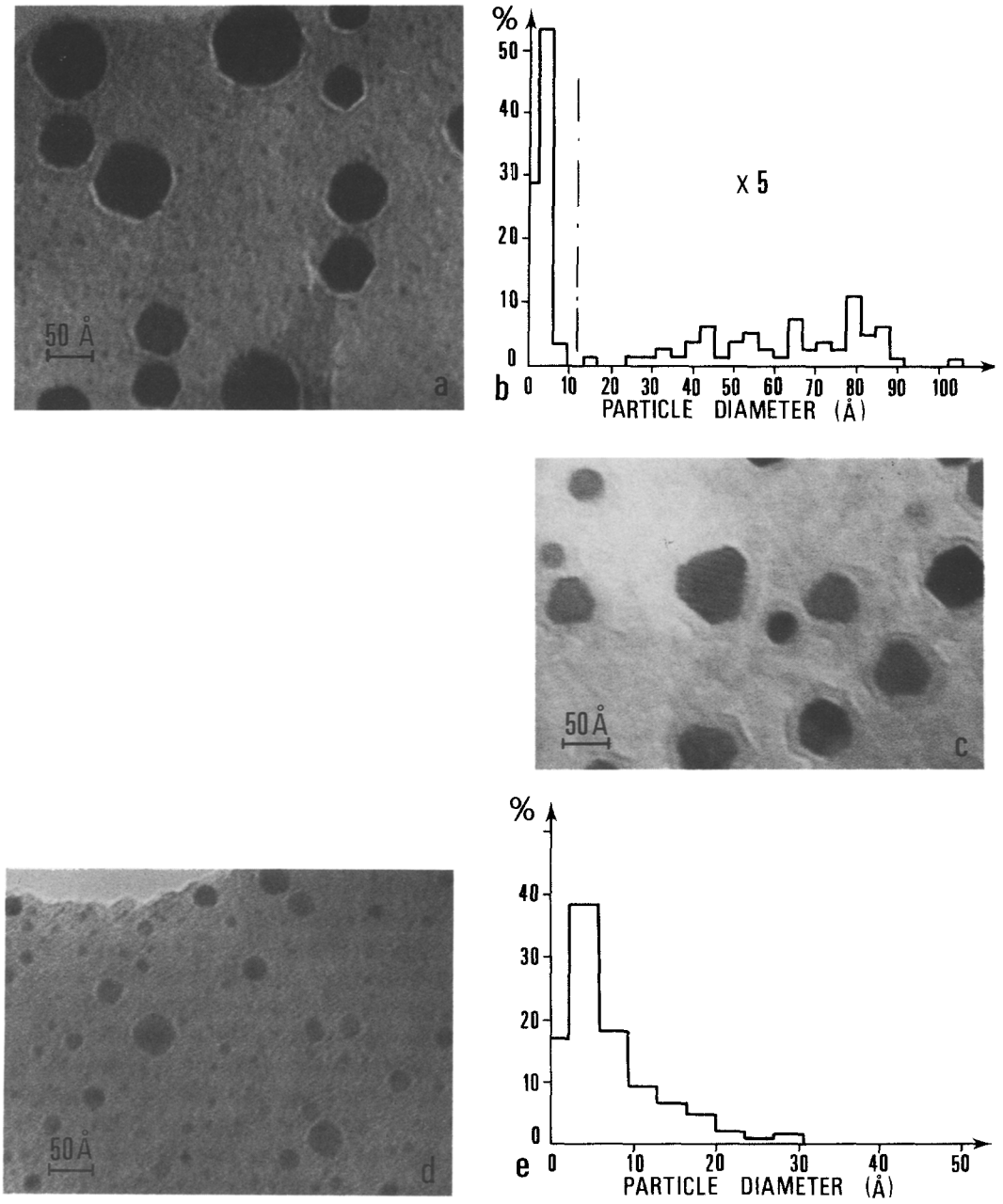

FIG. 3. Micrographs and corresponding size distributions of Pt/Al_2O_3 deposits ($Q_{TEM} \sim 0.5$). (a and b) Deposit followed by an O_2 treatment (20 Torr, 500°C, 1 h). (c) Previous treatment followed by H_2 reduction (1 Torr, 420°C, 1 h); example of moiré fringes. (d and e) Thinner Pt/Al_2O_3 deposit ($Q_{TEM} \sim 0.2$) treated in O_2 (20 Torr, 460°C, 1 h).

TABLE 2

Data Obtained Using AES (Peak-to-Peak Intensity I_d for $Pt_{153\ eV}$, I_s for $Al_{48\ eV}$) and Microscopy (Mean Diameter $\bar{d}$) on Similar Platinum Deposits Resulting from Different Treatments ($Q_{TEM} \sim 0.5$ Monolayer)

Treatments (1 h)	AES peak-to-peak height (a.u.)		Microscopy	
	I_d (Pt)	I_s (Al)	$\bar{d}$ (Å)	Diffraction
Pt deposit	2	3	20	Pt ring
Under vacuum at 500°C	Unchanged		20	Pt ring
Under N_2 ambient at 500°C	Unchanged		20	Pt ring
20 Torr O_2, $T < 450$°C	1.3	10	Weak contrast	Diffuse ring
20 Torr O_2, $T = 500$°C	0.2	10	<10 Å and >30 Å (bimodal distribution)	Pt ring
1 Torr O_2, $T = 550$°C	0.2	10	From 5 Å to 40 Å (broad distribution)	Pt ring

evaporated platinum, the following experimental precautions were taken:

—The treatment chamber contained only the heating holder with its platinum filament.

—Before each experiment, each sample was observed in TEM; through-focus series were taken to make sure there were no visible clusters due to ionic etching during sample preparation.

—A counterexperiment was performed, without any Pt deposit; the Al_2O_3 surface treated under the same conditions (preparation and O_2 treatment) remained unchanged as ascertained by microscopy and AES, and no trace of small clusters was visible (Fig. 2c).

In our presentation of the results, treatment under O_2 carried out at $T < 450$°C will be analysed separately from treatments performed in the temperature range 450–550°C.

(*a*) *Temperature lower than 450°C.* The micrograph of Fig. 2d shows the results of a treatment under 20 Torr O_2, 1 h, 420°C. The size and density of grains varied little, although some became less contrasted and partly vanished into the substrate, and others became slightly larger; the diffraction rings of platinum deposit, which were already weak, became even weaker. The Pt(153-eV) Auger signal decreased by 30 to 40% whatever the pressure (between 1 Torr and 1 atm), and the oxygen peak increased. More surprisingly, the Al peak, which was attenuated by the deposit, increased again until its intensity and position (eV) approached those of the bare substrate, whereas the uncovered surface of Al_2O_3 (as observed under TEM) hardly increased. These data indicate that Pt crystallites reacted with the substrate without undergoing any size variations.

(*b*) *Treatments between 460 and 550°C for 1 h.* A very different result was obtained here (Figs. 2e, 2f, and 3), involving considerable particle transformation.

(i) When the pressure was only 1 Torr, the treatment at 550°C was shown by TEM to lead to a broadening of the particle size distribution, in the size range 50 Å down to a peak of very small clusters of about 5 Å (Figs. 2e and 2f). The histogram represents all the particle sizes in the range 5 to 50 Å. Many particles exhibited a faceted shape or moiré fringes with substrate indicating that these were crystallites.

(ii) Under higher pressures, the treatment at 500°C, 20 Torr, for 1 h led to a bimodal size distribution, with particles in the size range 30 to 100 Å and numerous clusters

with diameters down to 5 to 10 Å in the case of the most visible clusters (Fig. 3a). In the example presented, the density of the smaller clusters was similar to the initial particle density, i.e., about six times higher than that of the larger particles. The latter were often shape faceted, sometimes twinned, and sometimes had moiré fringes (Fig. 3c).

In this micrograph the faceted platinum crystals have a low contrasted "envelope." We cannot explain this kind of image. This envelope has nothing to do with any focus effect. It has been found sometimes only after hydrogen treatment. It may be due to some contamination effect which is not present when the sample was only oxygen-treated.

In the electron diffraction patterns, the first four rings of platinum were always thinner and more intense than with the initial deposit. On the other hand, the two main rings of oxides PtO, PtO_2, or Pt_3O_4 were missing, if their intensity were high enough these rings should have been visible because the interplanar distances of these oxides differ by 0.2 Å from that of platinum (error on distance measurements within ±0.02 Å). The Al_2O_3 surface became amorphous due to the ion bombardment; therefore the crystallites could not have an epitaxial orientation, contrary to the results obtained on mica or NaCl single-crystal substrates (*31*). In an additional experiment the O_2 treatment was followed by a reduction using H_2 at 1 Torr, 420°C for 1 h (as is usual with catalyst preparation) without any significant changes in morphology or size distribution occurring. With a lower initial deposit $Q_{TEM} = 0.2$ (instead of 0.5) with a treatment similar to the above, the growth of the initially small particles (12 Å) was less conspicuous (35 Å maximum), but the small clusters were again very numerous (Figs. 3d and 3c).

For all the samples treated at around 500°C a noteworthy result was observed in AES: the Pt(153-eV) peak nearly disappeared and its intensity (reduced by 90%) was much lower than that which might be expected on the surface of the visible particles (coverage θ_{TEM} reduction < 50%; see Table 2).

DISCUSSION

These experiments show the essential difference between H_2 and N_2 treatments on the one hand and O_2 treatments on the other hand: the former have no significant effect on platinum particles, but in O_2 and under particular temperature and pressure conditions, a complete transformation of the grains takes place. These conditions were chosen to match closely those of commercial catalyst regeneration treatments; referring to Berry's diagram (P_{O_2}, T) (*32*) established for platinum ribbon oxidation (Fig. 4), we distinguished two treatment domains:

(i) one domain where the oxidation rate was maximum, i.e., with 20 Torr O_2 and a temperature of around 400°C; no significant size modification occurred here, but rather volumic grain transformations involving substrate interactions.

(ii) another at the edge between the oxidation domain and the oxide dissociation domain (500°C, 20 Torr), or in the latter; here the particles became larger than those at deposit, but also a population of very small clusters (<10 Å) appeared.

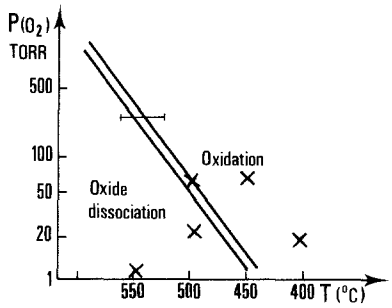

FIG. 4. Oxide dissociation pressure versus temperature curve for a platinum ribbon (from Ref. (*32*)). (X) (T, P) domain investigated in this article. (—) (T, P) domain used in industry for catalyst regeneration. (1 Torr = 133.3 Nm^{-2}.)

Owing to the precautions taken and to the counterexperiment (see paragraph 3 under Results), these small clusters necessarily originated from the initial platinum particles. In order to confirm that these small clusters contain platinum we have performed X-ray microanalysis with a TEM JEOL 2000FX operating at 200 kV with a probe size of 5 nm. When a 50-nm-diameter region, containing only these small clusters, was analysed, the platinum X-ray emission lines M_α and L_α appeared with an intensity which could be compared to that emitted from neighbouring large particles. The number of Pt atoms determined in this way appeared to be in agreement with the size of the small clusters determined from the micrographs. Other than Pt no additional element was detected on the sample. To make sure that the Pt signal from small clusters was not an artifact, we have looked for a 200-nm region on the sample without large and small clusters. In this region, the Pt X-ray signal remained negligible (ten times smaller than that on the first region, although the Al peak areas were similar).

The larger particles have a platinum core as shown by electron diffraction, but the composition of the clusters is unknown and further experiments will be necessary to establish it. From some micrographs it seems that the clusters are situated not only on the substrate but also on top or underneath some of the largest particles. One might assume that these small clusters may have been evaporated during the deposit and that, penetrating into the substrate, they did not participte in the surface particle growth during the deposit; the O_2 treatment would make them visible.

This last hypothesis does not however account for the experiment with weaker treatment (1 Torr), which did not show two modes of grains sizes, but all the sizes ranging between 5 and 50 Å (therefore with some particles growing and others diminishing) and with a smaller proportion of small clusters (Fig. 2e). This rather suggests that a transformation mechanism involving molecular migration may have taken place affecting all the particles. The matter transfer mechanism as well as the nature of the small clusters will be discussed below.

Matter Transfer by Molecular Migration

(*a*) *The molecular migration hypothesis.* This hypothesis might account for the decrease in the size of some grains and the growth of some others; atoms or molecules might be emitted and received by the particles, with a positive balance in the case of those which coarsen and a negative balance in the case of those which diminish. Variable duration treatments with which various stages of increase and decrease can be observed are required in order to confirm this assumption. However, with the classical Ostwald ripening process, the smaller particles decrease until they completely disappear (*33, 34*). This mechanism alone thus cannot explain the presence of a stable small cluster population on our catalysts. However, it is possible that once a small enough particle size has been reached, their interaction with the support or their composition is such that they cease to be transformed. However, the distribution of these clusters is more inhomogeneous than that of the deposit particles; in addition a portion of this population might not be visible. These small clusters may then consist either of initial particle residues or of visible remnants of mass transfer.

(*b*) *Particle mobility.* Among the two transfer processes with which any particle growth can be explained (crystallite migration and molecular migration), the migration coalescence of grains seems to have intervened rather little in our experiments; no grain gathering was observed as in the case of a carbon deposit on Al_2O_3 (after air treatment). The crystallite mobility on a carbon film (*35–37*) stands in contrast with the well-known immobility on clean alumina (*36*). The stability agrees with the slightness of the effects of UHV annealing (see paragraph 2 under Results). An oxidation might modify this immobility, but one

would have to assume that the oxidation was limited to a thin film not detected in diffraction; this surface oxidation assumption at 500°C leading to mobility seems to be in contradiction with the likely oxidation of grains and the immobility observed at 420°C (Results, paragraph 3a). Moreover, an increase in the adhesion of platinum films onto Al_2O_3 after heating in O_2 has recently been reported (*38*); Al atom diffusion through the Pt film is thought to be responsible for this stronger adhesion. Furthermore, the results of an experiment involving successive treatments (1 h) and observation of the same place in microscopy do not support the mobility hypothesis; none of the selected particles observed after 1 h in O_2 moved during the subsequent treatments. Above all, the mobility hypothesis does not explain the decrease in size of some of the particles.

(*c*) *The role of oxidation.* One can calculate the Pt atom coverage θ_{at} emitted at T = 500°C by a collection of platinum particles with a mean radius $\bar{r}$ = 15 Å, volume $\bar{v}$, in equilibrium with the mean vapour pressure $P(r)$, for a substance tension σ = 2300 ergs/cm^2 (*39*), an adsorption energy Pt atom–substrate $\Delta H_{ad} \simeq 2$ eV (*40*), and the vaporization energy $\Delta H_v^\circ \simeq 6$ eV (*27*):

$$\theta_m = \exp - \left(\Delta H_v^\circ - \Delta H_{ad} - \frac{2\bar{v}\sigma}{\bar{r}}\right) \Big/ kT$$

(see Ref. (*41*)). The coverage calculated with this relation is absolutely negligible ($<10^{-15}$) and cannot account for the quantity of matter transferred in 1 h (Fig. 2e), which is estimated to be $\sim 2.10^{-3}$ monolayer/s. This result agrees with the Pt/Al_2O_3 system stability observed under vacuum (*36*), as in the case of Pd/MgO (*42*). Now a simple O_2 adsorption which would decrease σ would also lower the Pt coverage θ_{at}. Thus it is unlikely that an Ostwald ripening operates between Pt particles. The transfer process is more likely to involve a superficial oxidation of platinum, decreasing ΔH_v° down to 2 eV for PtO_2 (*43, 32*) and leading to a more realistic coverage of 2.10^{-1} monolayer.

Ostwald ripening is certainly favoured under oxygen atmosphere as has indeed been observed; the platinum crystallites increase their size to the detriment of the smallest crystallites and these large crystallites facet under oxygen. This faceting is more pronounced after hydrogen treatment. However, the formation of the smallest clusters cannot be explained by Ostwald ripening, if we assume that they are in the same phase (e.g., platinum) as the large crystallites. The small clusters could be Pt oxide that would be visible in TEM. A possible formation mechanism could be as follows.

The Al_2O_3 single-crystal substrate being made amorphous at the surface by ion-bombardment during the cleaning procedure, it is conceivable that in addition to the Pt clusters (visible by TEM) nucleating on the surface some Pt atoms could diffuse inside the amorphous layer and bind to Al atoms. The modification of the Al Auger line could be explained in this way.

An O_2 treatment could result in the separation of the Pt from Al and favour the formation of a Pt oxide if the conditions (P, T) are fulfilled. Experimental results show that these conditions are necessary to see (by TEM) the small clusters. We have proved that these small clusters contain some Pt. In addition we have shown that the original Al Auger signal was restored after this treatment.

The next step of the explanation is that a hydrogen treatment could reduce the small oxide clusters to metallic Pt. However, at this stage small clusters are no longer visible. Does this reduced Pt become bidimensional as claimed by Yao *et al.* (*44, 45*), does it join the large Pt clusters by Ostwald ripening, or does it become atomically dispersed on special sites in the amorphous alumina layer? Further studies, with suitable techniques, could give additional information supporting one or another of these explanations.

CONCLUSION

Electron microscopy data show that model catalyst particles (Pt/Al_2O_3) in O_2 (500°C, 20 Torr, 1 h) are transformed into two phases; one involves Pt particles larger than the initial size and the other small clusters (<10 Å). This finding was made possible owing to the good transparency to the electrons of the alumina single crystals and owing to the contrast between Pt and Al_2O_3. It solves the apparent contradiction between the chemisorption measurements (hitherto interpreted as a catalyst redispersion in O_2) and the microscopic data on grain sintering.

ACKNOWLEDGMENTS

The authors thank Professor R. Kern for many fruitful discussions. The technical assistance of A. Ranguis is greatly acknowledged.

REFERENCES

1. McHenry, K. W., Bertolacini, R. J., Brennan, M. M., Wilson, J. L., and Seeling H. S., *in* "Proceedings, 2nd International Congress on Catalysis, Paris, 1960," p. 2295. Technip, Paris, 1961.
2. Johnson, M., and Keith, C., *J. Phys. Chem.* **67,** 200 (1963).
3. Coe, R. H., and Randlett, M. E., U.S. Patent Office 3, **278,** 419 (1966).
4. Mills, G. A., Weller, S., and Cornelius, E. B., *in* "Proceedings, 2nd International Congress on Catalysis, Paris, 1960," Vol. II, p. 2221. Technip, Paris, 1961.
5. Gruber, H. L., *J. Phys. Chem.* **66,** 48 (1962).
6. Menon, P. G., and Froment, G. F., *J. Catal.* **59,** 138 (1979).
7. Straguzzi, G. I., Aduriz, H. R., and Gigola, C. E., *J. Catal.* **66,** 171 (1980).
8. Adler, S. F., and Keavney, J. J., *J. Phys. Chem.* **64,** 208 (1960).
9. Gonzalez-Tejuca, L., Alka, K., Namba, S., and Turkevich, J., *J. Phys. Chem.* **81,** 1399 (1977).
10. Damiani, D. E., and Butt, J. B., *J. Catal.* **94,** 203 (1985).
11. Della Betta, R. A., McCune, R. C., and Sprys, J. W., *Ind. Eng. Chem. Proc. Res. Devel.* **15,** 169 (1976).
12. Tae Jin Lee and Young Gul Kim, *J. Catal.* **90,** 279 (1984).
13. Nakamura, M., Yamada, M., and Amano, A., *J. Catal.* **39,** 125 (1975).
14. Fiedorov, R., and Wanke, S., *J. Catal.* **43,** 34 (1976).
15. Dautzenberg, F. M., and Volters, H. B. M., *J. Catal.* **51,** 26 (1978).
16. Chu, Y. F., and Ruckenstein, E., *J. Catal.* **55,** 281 (1978).
17. Glassl, H., Hayek, K., and Kramer, R., *J. Catal.* **68,** 38 (1981).
18. Harris, P. J. F., Boyes, E. D., and Cairns, J. A., *J. Catal.* **82,** 127 (1983).
19. White, D., Baird, T., Fryer, J. R., Freeman, L. A., Smith, D. J., and Day, M., *J. Catal.* **81,** 119 (1983).
20. Smith, D. J., White, D., Baird, T., and Fryer, J. R., *J. Catal.* **81,** 107 (1983).
21. Stulga, J. E., Wynblatt, P., and Tien, J. K., *J. Catal.* **62,** 59 (1980).
22. Handbook of Auger Electron Spectroscopy, Perkin–Elmer Corporation, MN.
23. Carriere, B., Thèse Doctorat d'Etat, Strasbourg, 1977.
24. Poppa, H., and Soria, F., *Surf. Sci.* **115,** L105 (1982).
25. Sachtler, J. W. A., Van Hove, M. A., Biberian, J. P., and Somorjai, G. A., *Surf. Sci.* **110,** 19 (1981).
26. Kuijers, F. J., and Ponec, V., *Appl. Surf. Sci.* **2,** 43 (1978).
27. Honig, R. E., *RCA Rev.* 568 (1962).
28. Chemam, A., Thèse Université Aix-Marseille III, 1986.
29. Anton, R., Harsdorff, M., Paunov, M., and Schmeisser, H., *J. Appl. Phys. Suppl.* **2,** 1 (1974).
30. Reichelt, K., Lampert, B., and Siegers, H. P., *Surf. Sci.* **93,** 159 (1980).
31. Renou, A., et Gillet, M., *Thin Solid Films* **41,** 15 (1977).
32. Berry, R. J., *Surf. Sci.* **76,** 415 (1978).
33. Dadyburjor, D. B., and Ruckenstein, E., *J. Cryst. Growth* **40,** 279 (1977).
34. Chakraverty, B. K., *J. Phys. Chem. Solids* **28,** 2401 (1967).
35. Bett, J. A., Kinoshita, K., and Stonehart, P., *J. Catal.* **35,** 307 (1974).
36. Arai, M., Ishikawa, T., Nakayama, T., and Nishiyama, Y., *J. Colloid Interface Sci.* **97**(1), 254 (1984).
37. Chu, Y. F., and Ruckenstein, E., *Surf. Sci.* **67,** 517 (1977).
38. Budhani R. C., Prakash, S., Doerr, H. J., and Bunshah, R. F., *J. Vac. Sci. Technol. A* **4**(6), 3023 (1986).
39. Blakely J. M., and Maja, P. S., "Surfaces and Interfaces," p. 325. Syracuse Univ. Press, Syracuse, NY (1967).
40. McLean M., and Hondros, E. D., *J. Mater. Sci.* **6,** 19 (1971).

41. Kern, R., Le Lay, G., and Metois, J. J., *in* "Current Topics in Material Science," (E. Kaldis, Ed.), Vol 3, p. 128, Elsevier–North Holland, Amsterdam, 1979.
42. Heinemann, K., Osaka, T., Poppa, H., and Avalos-Borja, M., *J. Catal.* **83,** 61 (1983).
43. Samsonov, G. V., "The Oxide Handbook," p. 42. Plenum, New York, 1973.
44. Yao, H. C., Sieg, M., and Plummer, H. K., Jr., *J. Catal.* **59,** 365 (1979).
45. Yao, H. C., Japar, S., and Shelef, M., *J. Catal.* **50,** 407 (1977).